CANADIAN APPLIED MATHEMATICS QUARTERLY
Volume 0, Number 0, Preprint

A SEQUENTIAL SPECTRAL METHOD FOR NONLINEAR ELLIPTIC INTEGRO-DIFFERENTIAL EQUATIONS

M. J. Gander[1], A. Mansoora[2], K. K. Tam[3]

Abstract. A sequential spectral method (SSM) is a spectral method in which the unknown coefficients of the approximate spectral expansion are computed sequentially, one at a time, instead of simultaneously, like in a classical spectral method (CSM). These methods are especially suited for approximating difficult nonlinear integro-differential equations where the solution behavior is largely unknown and the problem lies in finding a solution of the large scale nonlinear system of equations for the unknown expansion coefficients. The SSM leads by iteration to the same solution as the underlying CSM and thus inherits its spectral accuracy, but it avoids the simultaneous solution of a large system of nonlinear equations. We prove convergence of the SSM to the spectral approximation of the underlying spectral method for a general class of nonlinear elliptic integro-differential equations, and illustrate the effectiveness of the method on two applications.

1. Introduction. We present an algorithm to solve nonlinear elliptic boundary value problems of the form

$$\begin{aligned} \mathcal{L}u &:= \Delta u + F(u) = 0, && \text{in } \Omega, \\ \mathcal{B}u &:= r\frac{\partial u}{\partial n} + su = 0, && \text{on } \partial\Omega, \end{aligned} \tag{1.1}$$

where $\frac{\partial}{\partial n}$ denotes the outward normal derivative on $\partial\Omega$, the boundary of Ω. The functions $r(\mathbf{x})$ and $s(\mathbf{x})$ in the boundary conditions are nonnegative and allow us to consider general Dirichlet, Neumann or Robin problems. The function $F(u)$ is a nonlinear function of u which can contain spatial integrals of some nonlinear functions of u.

The solution of problem (1.1) is in general obtained numerically using some form of discretization. Spectral methods are used if high accuracy is desired and the domain Ω is simple so that the set of eigenfunctions associated with the Laplacian, the domain and the boundary conditions can be obtained easily. This is often the case when the fundamental behavior of an equation is to be studied and the domain is not so important. Newer spectral methods can however deal with more general domains and boundary conditions, see for example [24], and have found their way into applications, see [10, 15] and references therein. In the spectral method we consider in this paper, the solution is sought as an infinite expansion in eigenfunctions. The coefficients in the expansion are determined by solving an infinite (in practice truncated) system of algebraic equations obtained by using a closure condition which, using a Galerkin

[1] McGill University, mgander@math.mcgill.ca
[2] McGill University, mansoora@math.mcgill.ca
[3] McGill University, tam@math.mcgill.ca

approach, is that the residual of the expansion has zero projection on the eigenfunctions. Solving these equations with Newton's method or a variant thereof [3] can be difficult and one often needs a good initial guess for the methods to converge. Also there might be multiple solutions and it is often difficult to detect this.

Tam et al. introduced in [22] a sequential approach to solve the resulting system of nonlinear equations for a semi-linear elliptic partial differential equation. We call this method a sequential spectral method (SSM). In contrast to a classical spectral method (CSM), where the coefficients are determined simultaneously by solving a system of nonlinear equations, in the SSM the coefficients are determined sequentially by solving a single equation at each step, and through iteration, convergence to the approximate solution of the CSM is achieved. The sequential nature of the computations makes the size of the system somewhat immaterial, as only a single equation is solved at any stage of the procedure. The SSM has been applied to nonlinear integral equations in [23], to parabolic partial differential equations in [1, 18, 2], and to the Navier-Stokes equation in [13]. Independently, a more general frequency decomposition and subspace correction algorithm for an abstract parabolic evolution equation has been proposed and analyzed in [11], see also [12].

We analyze in this paper the convergence of the SSM applied to nonlinear elliptic integro-differential equations. We develop the method in Section 2, analyze its convergence behavior in Section 3 and illustrate its performance in Section 4 on a problem from combustion theory and a problem from shear banding.

2. The Sequential Spectral Method. We develop the SSM for problem (1.1). Let $\{\lambda_j\}$ be the eigenvalues and $\{\phi_j(\mathbf{x})\}$ be the orthonormal eigenfunctions of the Laplacian,

$$\Delta\phi_j = -\lambda_j\phi_j, \quad \text{in } \Omega, \tag{2.1}$$

where the eigenfunctions $\{\phi_j(\mathbf{x})\}$ satisfy homogeneous boundary conditions of Dirichlet, Neumann and/or Robin type. For all combinations, except for the pure Neumann case, there is no zero eigenvalue. We assume in the sequel that $\lambda_j > 0$ and treat the pure Neumann case where a zero eigenvalue is present separately at the end of Section 3. Our analysis is in $L^2(\Omega)$, with the associated inner product $(u,v) = \int_\Omega u(\mathbf{x})v(\mathbf{x})d\mathbf{x}$ for $u, v \in L^2(\Omega)$ and we assume that $F : L^2(\Omega) \mapsto L^2(\Omega)$. Note that this does not guarantee existence of a solution for problem (1.1). To prove convergence of the SSM, we will later introduce an additional condition, and with this condition the convergence analysis of the SSM provides also an existence proof of solutions for (1.1).

The SSM we present here consists of two parts: first, a good initial guess $u^{(0)}$ is constructed solving only scalar nonlinear equations at each step. Second, an iteration solving only scalar linear equations at each step is used to obtain an approximate solution, starting with this initial guess. Other combinations of scalar linear and nonlinear solves would also be possible in the framework of the SSM, see [12, 13].

2.1. The Initial Guess for the SSM. To simplify notation, we use the generic symbol $\tilde{u}(\mathbf{x})$ to denote an approximation to $u(\mathbf{x})$ when constructing the initial guess in this subsection. We first set $\tilde{u}(\mathbf{x}) := a_1\phi_1(\mathbf{x})$ and compute the residual

$$R(\tilde{u}) = -\lambda_1 a_1\phi_1 + F(a_1\phi_1). \tag{2.2}$$

Using the Galerkin closure condition, the projection of $R(\tilde{u})$ onto the first eigenfunction ϕ_1 needs to vanish, $(R(\tilde{u}), \phi_1) = 0$, which leads to the nonlinear scalar equation

$$-\lambda_1 a_1 + (F(a_1\phi_1), \phi_1) = 0 \tag{2.3}$$

for a_1. This equation may have multiple solutions, in which case each solution a_1 can generate an expansion for a solution $u(\mathbf{x})$ of problem (1.1). To proceed, we focus on one solution. With a_1 determined, we set $\tilde{u}(\mathbf{x}) := a_1\phi_1(\mathbf{x}) + a_2\phi_2(\mathbf{x})$ and compute again the residual,

$$R(\tilde{u}) = -\lambda_1 a_1\phi_1 - \lambda_2 a_2\phi_2 + F(a_1\phi_1 + a_2\phi_2).$$

Now, we require $(R(\tilde{u}), \phi_2) = 0$, and using the orthonormality of the eigenfunctions, we get the scalar nonlinear equation

$$-\lambda_2 a_2 + (F(a_1\phi_1 + a_2\phi_2), \phi_2) = 0 \tag{2.4}$$

for a_2. Equation (2.4) may have more than one solution, in which case we have to take one at a time.

Proceeding in this manner, we generate a sequence of coefficients $\{a_j\}$, and consider formally the approximation $\tilde{u}(\mathbf{x}) := \sum_{j=1}^{\infty} a_j\phi_j(\mathbf{x})$. We have the residual

$$R(\tilde{u}) = -\sum_{j=1}^{\infty} \lambda_j a_j\phi_j + F(\sum_{j=1}^{\infty} a_j\phi_j). \tag{2.5}$$

Now using the completeness of the eigenfunctions, we expand F into eigenfunctions,

$$F(\sum_{j=1}^{\infty} a_j\phi_j) = \sum_{k=1}^{\infty} b_k\phi_k(\mathbf{x}), \tag{2.6}$$

where the coefficients b_k are given by $b_k = (F(\sum_{j=1}^{\infty} a_j\phi_j), \phi_k)$. The residual in (2.5) then becomes

$$R(\tilde{u}) = \sum_{j=1}^{\infty} (-\lambda_j a_j + b_j)\phi_j. \tag{2.7}$$

Now for $\tilde{u}(\mathbf{x})$ to be a solution, according to the Galerkin condition, the residual would need to vanish, $(R(\tilde{u}), \phi_j) = 0$ for all j, which would imply

$$\lambda_j a_j - b_j = 0, \qquad \text{for } j = 1, 2, \ldots. \tag{2.8}$$

Unfortunately our a_j just computed will usually not satisfy (2.8) and we need to introduce an iteration to achieve the required equality (2.8).

2.2. The SSM Iteration. Let $u^{(n)}(\mathbf{x})$ denote the nth approximation of $u(\mathbf{x})$, given by

$$u^{(n)}(\mathbf{x}) = \sum_{j=1}^{\infty} a_j^{(n)}\phi_j(\mathbf{x}), \tag{2.9}$$

and let $b_j^{(n)}$ be the coefficients in the expansion of F,

$$F(u^{(n)}(\mathbf{x})) = \sum_{j=1}^{\infty} b_j^{(n)} \phi_j(\mathbf{x}). \tag{2.10}$$

We construct a new sequence $\{a_j^{(n+1)}\}$ by setting

$$a_j^{(n+1)} = \frac{1}{\lambda_j} b_j^{(n)} = \frac{1}{\lambda_j} (F(u^{(n)}), \phi_j), \tag{2.11}$$

where we used that $\lambda_j > 0$. From (2.11) we construct the new approximation

$$u^{(n+1)}(\mathbf{x}) = \sum_{j=1}^{\infty} a_j^{(n+1)} \phi_j(\mathbf{x}). \tag{2.12}$$

If the SSM (2.9)-(2.12) converges, then $R(u^{(\infty)}) = 0$ and hence a solution of problem (1.1) is obtained.

3. Convergence Results. Our first convergence result is obtained without assuming existence of a solution. The convergent SSM establishes existence of a solution in that case.

Theorem 3.1 *Let $F : L^2(\Omega) \mapsto L^2(\Omega)$ be globally Lipschitz with Lipschitz constant L_F,*

$$||F(u) - F(v)||_2 \leq L_F ||u - v||_2, \quad \forall\ u, v \in L^2(\Omega),$$

and let λ_1 be the smallest positive eigenvalue of the eigenvalue problem (2.1). If

$$L_F < \lambda_1, \tag{3.1}$$

then the SSM (2.9)-(2.12) converges to a solution $u(\mathbf{x})$ of problem (1.1).

Proof. To show that the SSM is a contraction, let

$$g^{(n)}(\mathbf{x}) := F(u^{(n)}(\mathbf{x})) - F(u^{(n-1)}(\mathbf{x})) = \sum_{j=1}^{\infty} g_j^{(n)} \phi_j(\mathbf{x}), \tag{3.2}$$

where $g_j^{(n)}$ are the Fourier coefficients of $g^{(n)}(\mathbf{x}) := F(u^{(n)}(\mathbf{x})) - F(u^{(n-1)}(\mathbf{x}))$,

$$g_j^{(n)} = (g^{(n)}, \phi_j) = (F(u^{(n)}) - F(u^{(n-1)}), \phi_j). \tag{3.3}$$

Then the difference of corresponding coefficients a_j between two iteration steps is

$$a_j^{(n+1)} - a_j^{(n)} = \frac{1}{\lambda_j} \int_{\Omega} [F(u^{(n)}) - F(u^{(n-1)})] \phi_j d\mathbf{x} = \frac{1}{\lambda_j} g_j^{(n)}. \tag{3.4}$$

Multiplying both sides by $\phi_j(\mathbf{x})$, $j = 1, 2, 3, \ldots$ and summing over j we obtain

$$u^{(n+1)}(\mathbf{x}) - u^{(n)}(\mathbf{x}) = \sum_{j=1}^{\infty} \left(a_j^{(n+1)} - a_j^{(n)} \right) \phi_j(\mathbf{x}) = \sum_{j=1}^{\infty} \frac{g_j^{(n)}}{\lambda_j} \phi_j(\mathbf{x}). \tag{3.5}$$

Taking the L^2 norm squared on both sides and using Parseval's identity, we obtain

$$||u^{(n+1)} - u^{(n)}||_2^2 = \sum_{j=1}^{\infty} \left| \frac{g_j^{(n)}}{\lambda_j} \right|^2 \leq \frac{1}{\lambda_1^2} \sum_{j=1}^{\infty} |g_j^{(n)}|^2, \tag{3.6}$$

because the eigenvalues $\{\lambda_j\}$ are positive and increasing. Since $g_j^{(n)}$ are the Fourier coefficients of the function $g^{(n)}(\mathbf{x})$, using Parseval's identity again, we obtain

$$||u^{(n+1)} - u^{(n)}||_2^2 \leq \frac{1}{\lambda_1^2} ||g^{(n)}||_2^2 = \frac{1}{\lambda_1^2} ||F(u^{(n)}) - F(u^{(n-1)})||_2^2. \tag{3.7}$$

With the Lipschitz condition on F, we finally obtain, after taking the square-root,

$$||u^{(n+1)} - u^{(n)}||_2 \leq \frac{L_F}{\lambda_1} ||u^{(n)} - u^{(n-1)}||_2, \tag{3.8}$$

which proves that, if $L_F < \lambda_1$, then the sequence $\{u^{(n)}\}$ is a contraction in $L^2(\Omega)$ and hence converges. ■

The next result now uses the existence of a solution under the conditions of Theorem 3.1 to derive the convergence rate of the SSM and an a priori error estimate for the method.

Theorem 3.2 (Linear Convergence) *If F satisfies the hypotheses of Theorem 3.1, then the SSM (2.9)-(2.12) converges to a solution $u(\mathbf{x})$ of problem (1.1) at the linear rate*

$$||u - u^{(n)}||_2 \leq \left(\frac{L_F}{\lambda_1} \right)^n ||u - u^{(0)}||_2. \tag{3.9}$$

In addition, we have the a priori error estimate

$$||u - u^{(n)}||_2 \leq \frac{(\frac{L_F}{\lambda_1})^n}{1 - \frac{L_F}{\lambda_1}} ||u^{(1)} - u^{(0)}||_2. \tag{3.10}$$

Proof. To prove (3.9), let $u(\mathbf{x}) = \sum_{j=1}^{\infty} a_j \phi_j(\mathbf{x})$ be a solution of problem (1.1). Then, from (1.1), we have $\sum_{j=1}^{\infty} \lambda_j a_j \phi_j(\mathbf{x}) = F(u(\mathbf{x}))$, which implies $a_j = \frac{1}{\lambda_j}(F(u), \phi_j)$. Using the value of $a_j^{(n)}$ from equation (2.10), we get

$$a_j - a_j^{(n)} = \frac{1}{\lambda_j} \int_{\Omega} [F(u) - F(u^{(n)})] \phi_j d\mathbf{x}. \tag{3.11}$$

Following precisely the same steps as in Theorem 3.1, we obtain

$$||u - u^{(n)}||_2 \leq \frac{L_F}{\lambda_1} ||u - u^{(n-1)}||_2, \tag{3.12}$$

and by induction

$$||u - u^{(n)}||_2 \leq \left(\frac{L_F}{\lambda_1} \right)^n ||u - u^{(0)}||_2. \tag{3.13}$$

Since $\frac{L_F}{\lambda_1} < 1$, the sequence $\{u^{(n)}(\mathbf{x})\}$ converges linearly to $u(\mathbf{x})$ in $L^2(\Omega)$. To show the a priori error estimate (3.10), we have, using inequality (3.8) recursively,

$$||u^{(n+1)} - u^{(n)}||_2 \leq \frac{L_F}{\lambda_1}||u^{(n)} - u^{(n-1)}||_2 \leq \cdots \leq \left(\frac{L_F}{\lambda_1}\right)^n ||u^{(1)} - u^{(0)}||_2.$$

For $m > n$, we have

$$\begin{aligned}||u^{(m)} - u^{(n)}||_2 &\leq ||u^{(m)} - u^{(m-1)}||_2 + ||u^{(m-1)} - u^{(m-2)}||_2 + \cdots + ||u^{(n+1)} - u^{(n)}||_2 \\ &\leq \left(\frac{L_F}{\lambda_1}\right)^{m-1} ||u^{(1)} - u^{(0)}||_2 + \cdots + \left(\frac{L_F}{\lambda_1}\right)^n ||u^{(1)} - u^{(0)}||_2 \\ &= \left(\frac{L_F}{\lambda_1}\right)^n \left[\left(\frac{L_F}{\lambda_1}\right)^{m-n-1} + \left(\frac{L_F}{\lambda_1}\right)^{m-n-2} + \cdots + \frac{L_F}{\lambda_1} + 1\right] ||u^{(1)} - u^{(0)}||_2.\end{aligned}$$

The terms in the parenthesis form a geometric series, and $\lim_{m\to\infty} u^{(m)} = u$, so

$$\begin{aligned}||u - u^{(n)}||_2 = \lim_{m\to\infty} ||u^{(m)} - u^{(n)}||_2 &\leq \left(\frac{L_F}{\lambda_1}\right)^n ||u^{(1)} - u^{(0)}||_2 \sum_{j=0}^{\infty} \left(\frac{L_F}{\lambda_1}\right)^j \\ &= \frac{(\frac{L_F}{\lambda_1})^n}{1 - \frac{L_F}{\lambda_1}} ||u^{(1)} - u^{(0)}||_2,\end{aligned}$$

which gives the a priori error bound. ■

In Theorem 3.1, we assume F to be globally Lipschitz in $L^2(\Omega)$. From relation (3.9), we see however that all iterates stay in a ball $B(u, r)$, centered at the solution u, with radius $r = ||u - u^{(0)}||_2$. So we can relax the global Lipschitz condition which leads to the following corollary.

Corollary 3.1 *Let F be locally Lipschitz in a ball $B(u, r)$, centered at the solution u, with radius $r = ||u - u^{(0)}||_2$, where $u^{(0)}$ is the initial guess, with Lipschitz constant L_F, and let λ_1 be the smallest positive eigenvalue of the eigenvalue problem (2.1). If $L_F < \lambda_1$, then the SSM converges linearly at the rate given in (3.9).*

Note that condition (3.1) on the ratio between the Lipschitz constant and the first eigenvalue of the underlying elliptic operator is a sufficient condition for convergence, but it is not necessary. The iteration may converge even if this condition is violated. In practice one can just run the algorithm and see whether convergence is achieved or not, one does not necessarily have to be able to check the Lipschitz condition.

We have so far excluded the case of pure Neumann conditions, since then problem (2.1) can have a zero eigenvalue and the SSM can not be defined because of equation (2.11). However, if $\lambda_1 = 0$ and the nonlinear function $F(u)$ is a combination of a linear function ζu, and a nonlinear function $F_1(u)$, that is,

$$F(u) = \zeta u + F_1(u), \tag{3.14}$$

then we can define the iteration scheme by

$$a_j^{(n+1)} = \frac{1}{(\lambda_j - \zeta)} (F_1(u^{(n)}), \phi_j), \tag{3.15}$$

provided $\zeta \neq \lambda_j$, $j = 1, 2, 3, \ldots$.

If $F_1(u)$ is Lipschitz in a ball which contains all iterates of $u^{(n)}$ with Lipschitz constant L_{F_1}, then the convergence analysis of the SSM follows in the same way and we obtain that if

$$L_{F_1} < \min_j |\lambda_j - \zeta|, \tag{3.16}$$

then the sequence $\{u^{(n)}\}$ is contractive.

4. Numerical Results. In practice, we truncate the infinite expansion and use a finite number N of eigenfunctions. The number of coefficients needed depends on the problem at hand and the required accuracy of the solution. We show numerical results for two integro-differential boundary value problems of the form (1.1); more numerical experiments and further applications can be found in [1, 18, 13, 12]. First, we consider the case

$$F(u) = \sigma \left(f_1(u) + b \int_\Omega f_2(u) d\mathbf{x} \right), \tag{4.1}$$

where b and σ are positive constants. The nonlinear functions $f_1(u)$ and $f_2(u)$ are locally Lipschitz with respect to u and convex, $f_1(0) > 0$, $f_2(0) > 0$, and $f_2(u)$ is increasing in u. Such problems arise in the thermal explosion process of a compressible reactive gas, see [4] and [21]. This form of $F(u)$ is considered in Subsection 4.1 and the convergence is fully analyzed in this case.

Second, we consider a nonlinear term of the form

$$F(u) = \frac{\delta f(u)}{(\int_\Omega f(u) d\mathbf{x})^p}, \tag{4.2}$$

where f is Lipschitz continuous and positive, and the parameters satisfy $p \geq 0$ and $\delta > 0$. Such nonlocal problems arise, for example, in the study of phenomena associated with the occurrence of shear bands in metals being deformed under high strain rates [8], [20], [7], in modeling the phenomena of Ohmic heating [16], [17], in the investigation of the fully turbulent behavior of a real flow, using invariant measures for the Euler equation [9], and in the theory of gravitational equilibrium of polytropic stars [14]. We solve an example of this form of $F(u)$ in Subsection 4.2 which illustrates the numerous advantages of the SSM over the corresponding CSM.

4.1. Combustion Theory. The governing equation for the steady state problem of thermal explosion in combustion theory is (see [21])

$$\begin{aligned} D u_{xx} + \sigma [e^{\gamma u} + b \int_0^1 e^{\gamma u(y)} dy] &= 0, \quad x \in (0,1), \\ u(0) = u(1) &= 0, \end{aligned} \tag{4.3}$$

where u is the temperature distribution of a gas, D, σ and γ are positive constants and b is a nonnegative gas constant. Here, σ is the Frank-Kamenetski parameter. The last term on the left hand side is due to the compressibility of the gas. Problem (4.3) is discussed by Pao in [21], and he proves that there exists a critical value of σ, denoted by σ^*, such that for $\sigma < \sigma^*$, the problem (4.3) has a positive solution, and for $\sigma > \sigma^*$, no positive solution can exist.

To prove convergence of the SSM applied to this problem we need the following Lemma.

	CSM	SSM	
j	a_j	$a_j^{(0)}$	$a_j^{(7)}$
1	0.1011161715	0.1010572002	0.1011161715
3	0.0035579473	0.0035576649	0.0035579473
5	0.0007665042	0.0007664819	0.0007665042
7	0.0002791390	0.0002791332	0.0002791390
9	0.0001312981	0.0001312960	0.0001312981
11	0.0000719033	0.0000719013	0.0000719033

Table 4.1: Comparison of the coefficients obtained by the CSM and the SSM.

Lemma 4.1 *Let $f_1 : L^2(\Omega) \mapsto L^2(\Omega)$ and $f_2 : L^2(\Omega) \mapsto L^2(\Omega)$ be Lipschitz with constants L_1 and L_2. Then $F(u) := \sigma\left(f_1(u) + b\int_\Omega f_2(u)d\mathbf{x}\right)$, with b and σ positive constants, is Lipschitz with constant $L_F = \sigma(L_1 + b|\Omega|L_2)$.*

Proof. For any $u, v \in L^2(\Omega)$, we have, using the triangle inequality

$$||F(u) - F(v)||_2 \le \sigma||f_1(u) - f_1(v)||_2 + \sigma b\sqrt{\int_\Omega \left|\int_\Omega [f_2(u) - f_2(v)]d\mathbf{x}\right|^2 d\mathbf{x}}.$$

Using the Cauchy-Schwarz inequality on the second term on the right we obtain

$$\left|\int_\Omega [f_2(u) - f_2(v)]d\mathbf{x}\right| = \left|\int_\Omega 1 \cdot [f_2(u) - f_2(v)]d\mathbf{x}\right| \le |\Omega|^{1/2}||f_2(u) - f_2(v)||_2$$

where $|\Omega|$ denotes the volume of Ω. The result now follows with the Lipschitz assumptions on f_1 and f_2. ∎

With this Lemma, Theorems 3.1 and 3.2 apply and hence the SSM converges for problem (4.3) if $\sigma(1+b)L_1 < \lambda_1$. We solve the problem numerically for the values $\sigma = 1/2$, $b = D = \gamma = 1$. The orthonormal eigenfunctions are $\phi_j = \sqrt{2}\sin(j\pi x)$, and the corresponding eigenvalues are $\lambda_j = j^2\pi^2$, $j = 1, 2, 3, \ldots$. Using the SSM, we find that the even Fourier coefficients satisfy numerically $|a_{2j}^{(0)}| < 10^{-20}$, so the a_j are important for odd values of j only. In fact the even coefficients vanish identically, which is proved for the parabolic case of problem (4.3) in [18], using the SSM. This information reduces the problem of solving a system of N nonlinear algebraic equations to a system of $\frac{N}{2}$ equations in the CSM. Note that this kind of observation can not be obtained directly using the CSM. Table 4.1 shows the numerical results obtained using the CSM and the SSM for $N = 11$. The results show that the initial coefficients $a_j^{(0)}$ of the SSM are very close to the coefficients a_j of the CSM, and in only 7 linear iterations the a_j converge to the classical spectral approximation to full precision. Figure 4.1 shows that there is a very small difference between the approximate solution obtained from the initial coefficients $a_j^{(0)}$ and the CSM coefficients a_j, $|u^c - u^{(0)}| \le 10^{-4}$ for all values of $x \in \Omega$.

By Lemma 4.1, the Lipschitz constant L_F for problem (4.3) is $L_F = e^{0.14}$, for $\sigma = 1/2$ and $b = D = \gamma = 1$. Therefore by Theorem 3.2, the convergence factor of the

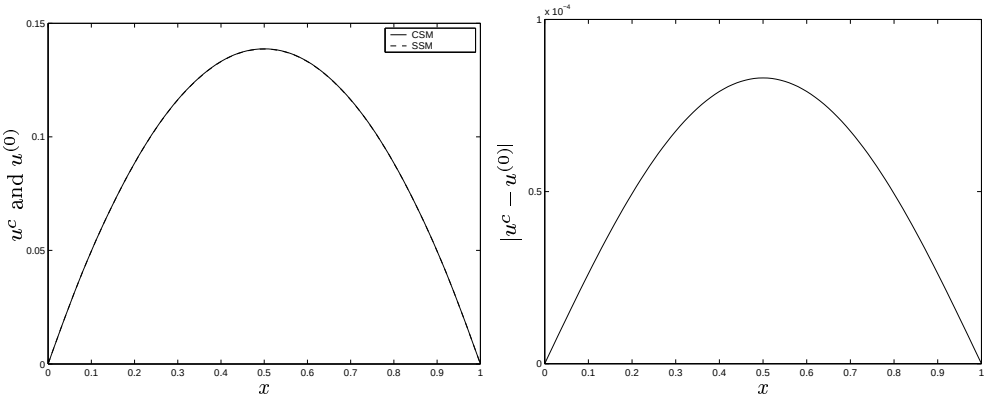

Figure 4.1: Comparison of $u^c = \sum_{j=1}^{11} a_j \phi_j$ and $u^{(0)} = \sum_{j=1}^{11} a_j^{(0)} \phi_j$ and the difference $|u^c - u^{(0)}|$.

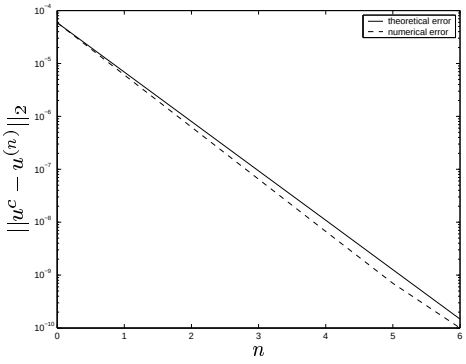

Figure 4.2: Comparison of the theoretical and actual error at the nth step. The SSM converges linearly.

SSM is $\frac{L_F}{\lambda_1} = 0.116547102$. Figure 4.2 shows very good agreement of the theoretical and the actually measured convergence rate.

Now we consider the problem (4.3) in 2 dimensions and solve it for the same values of the parameters, $\sigma = 1/2$, $b = D = \gamma = 1$. The orthonormal eigenfunctions are $\phi_{ij} = 2\sin(i\pi x)\sin(j\pi y)$ and the corresponding eigenvalues are $\lambda_{ij} = (i^2 + j^2)\pi^2$, $i, j = 1, 2, 3, \ldots$. Using the SSM, we find that the Fourier coefficients of the initial approximation satisfy numerically $|a_{ij}^{(0)}| < 10^{-20}$, if one or both of the i, j are even, so the a_{ij} seem to be relevant in the approximate solution for odd values of i and j only. Like in the one dimensional case, this observation from the SSM reduces the size of the nonlinear system to be solved considerably, and it would be difficult to make this kind of observation when using the CSM. Table 4.2 shows the numerical results obtained using the CSM and the SSM for $N = 5$. The results show that the initial coefficients $a_{ij}^{(0)}$ are very close to the classical spectral coefficients a_{ij} and in

	CSM	SSM	
ij	a_{ij}	$a_{ij}^{(0)}$	$a_{ij}^{(8)}$
11	0.0429559330	0.0429190549	0.0429559330
13	0.0028024720	0.0028010427	0.0028024720
31	0.0028024720	0.0028021133	0.0028024720
33	0.0005180161	0.0005179507	0.0005180161
15	0.0006447836	0.0006447370	0.0006447836
51	0.0006447836	0.0006447703	0.0006447836
35	0.0001643128	0.0001643097	0.0001643128
53	0.0001643128	0.0001643111	0.0001643128
55	0.0000670063	0.0000670052	0.0000670063

Table 4.2: Comparison of the coefficients obtained by the CSM and the SSM for the two dimensional case.

only 8 linear iterations the a_{ij} converge to the classical spectral approximation to full precision.

4.2. The Formation of Shear Bands in Materials. The formation of shear bands in metals has important implications to a variety of technological processes. These bands are observed in very thin zones and generally regarded as a precursor to material failure. Shear band formation is caused by the heat generated in regions with highest strain rate. With insufficient time for diffusion of this heat, a localized thermal softness of the metal occurs which enhances plastic flow in a thin zone. This localization of plastic strain into an adiabatic shear band during rapid plastic shear shares some interesting similarities with the ignition problem in combustion for chemically reactive systems.

Consider loading a thin walled tube of metal of length d in torsion with the ends held at constant temperature, the initial temperature of the tube. One end of the tube is fixed and the other end is twisted at a constant rate $v = v_0$. Then the mathematical model for the shearing process (a detailed derivation can be found in [5] or [7]) is given by the non-local parabolic problem

$$\frac{\partial u}{\partial t} - \frac{\partial^2 u}{\partial x^2} = \frac{\delta e^u}{(\int_{-1}^{1} e^u dx)^p}, \quad u(-1,t) = u(1,t) = 0, \quad u(x,0) = u_0(x) \geq 0, \tag{4.4}$$

where $\delta > 0$ and $p \geq 0$.

The nonlocal initial boundary value problem (4.4) appears to be very much like the classical ignition model for rigid reactive materials assuming one step Arrhenius chemistry and in fact reduces to the ignition model for $p = 0$. The model developed by Burns in [8] has $p = 1$. Burns' model has been studied in detail by Bebernes and Talaga in [7], and they have verified that a unique bounded solution exists for all $\delta > 0$. This implies that no shear banding occurs in Burns model. If, however, the model is given with $0 \leq p < 1$, then there exists a critical value δ^*, such that, for all $\delta > \delta^*$, the solutions blow up in finite time. This does predict shear banding as observed in experiments by Merchand and Duffy [19].

	CSM	SSM		CSM	SSM	
j	a_j	$a_j^{(0)}$	$a_j^{(6)}$	a_j	$a_j^{(0)}$	$a_j^{(6)}$
1	0.189173752	0.189561292	0.189173752	0.610427863	0.612456619	0.610427863
2	-0.005704984	-0.005705579	-0.005704984	-0.009285960	-0.009276831	-0.009285960
3	0.001228008	0.001227847	0.001228008	0.002380523	0.002379187	0.002380523
4	-0.000469654	-0.000446864	-0.000469654	-0.000878048	-0.000877113	-0.000878048
5	0.000210188	0.000210130	0.000210188	0.000415311	0.000414748	0.000415311
6	-0.000115091	-0.000115055	-0.000115091	-0.000228054	-0.000227697	-0.000228054
7	0.000069716	0.000069691	0.000069716	0.000138411	0.000138124	0.000138411
	$\delta = 1$			$\delta = 3$		

Table 4.3: Comparison of the coefficients obtained by the CSM and the SSM for $p = 1$ and $\delta = 1$ or $\delta = 3$.

The steady state problem associated with (4.4) is

$$-\frac{\partial^2 u}{\partial x^2} = \frac{\delta e^u}{(\int_{-1}^{1} e^u dx)^p}, \quad u(-1) = u(1) = 0. \tag{4.5}$$

From the classical theory of partial differential equations, any solution of the boundary value problem (4.5) is radially symmetric and radially decreasing [6]. So problem (4.5) can be written as

$$-\frac{\partial^2 u}{\partial x^2} = \frac{\delta e^u}{(2\int_{0}^{1} e^u dx)^p}, \quad u'(0) = 0, \quad u(1) = 0. \tag{4.6}$$

Bebernes and Lacey proved in [6] the following theorem.

Theorem 4.1 *If $p \geq 1$, then the boundary value problem (4.6) has a unique solution for all $\delta > 0$. If $0 \leq p < 1$, then there exists $\delta^* > 0$ such that the boundary value problem (4.6) has two solutions for $\delta < \delta^*$, one solution for $\delta = \delta^*$ and no solution for $\delta > \delta^*$.*

We examine the approximations of problem (4.6) for different values of p using the SSM and the CSM and compare the numerical results. From the eigenvalue problem

$$\frac{d^2\phi}{dx^2} = -\lambda\phi, \qquad \frac{d\phi}{dx}(0) = 0, \quad \phi(1) = 0,$$

we obtain the eigenvalues $\lambda_j = [\frac{(2j-1)\pi}{2}]^2$ and orthonormal eigenfunctions $\phi_j = \sqrt{2}\cos(\frac{(2j-1)\pi x}{2})$, $j = 1, 2, 3, \ldots$.

For $p = 1$, we obtain with the SSM a unique solution for all values of $\delta > 0$ as expected. Table 4.3 shows the values of the coefficients $a_j^{(n)}$ from the SSM and a_j from the CSM for $\delta = 1$ and $\delta = 3$. The coefficients $a_j^{(0)}$ are found using bisection and the classical spectral coefficients a_j are obtained using the nonlinear equation solver in Maple with tolerance 10^{-10}, using as an initial guess the one computed with the SSM. Without this initial guess, the Maple solver has difficulties to find the solution of

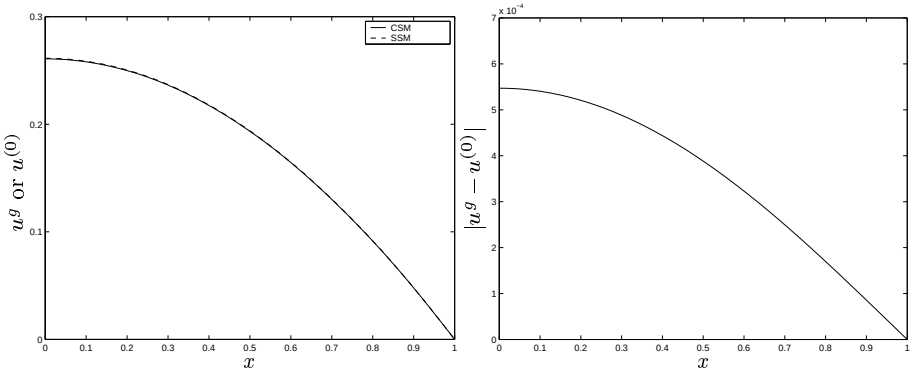

Figure 4.3: Comparison of u^c and $u^{(0)}$, and the difference $|u^c - u^{(0)}|$ for $p = 1$ and $\delta = 1$.

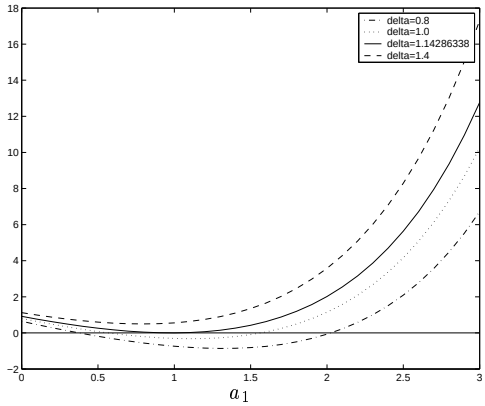

Figure 4.4: Solutions for $a_1^{(0)}$ of equation (4.7) for $p = 1/6$ and for different values of δ, where $\delta^* \approx 1.14286338$.

the nonlinear system numerically. In Figure 4.3, we show the spectral approximation $u^c = \sum_{j=1}^{7} a_j \phi_j(x)$ and the initial approximation $u^{(0)} = \sum_{j=1}^{7} a_j^{(0)} \phi_j(x)$ from the SSM, and the difference $|u^c - u^{(0)}|$. We see from the figures and tables that the $a_j^{(0)}$ are very close to the classical spectral coefficients a_j and converge to a_j in only a few iterations. Table 4.3 also shows that the coefficients a_j become smaller when j increases. This is one of the great features of spectral methods which leads to the well known spectral accuracy. While using the SSM, we can use this decaying property of the coefficients to determine N on the fly, which is not possible in the CSM, where the system size has to be determined in advance.

For $0 \le p < 1$, we find with the SSM that the first equation to be solved for $a_1^{(0)}$ is

$$-\frac{\pi^2}{4} a_1^{(0)} + \frac{\delta\sqrt{2}\int_0^1 e^{\sqrt{2}\, a_1^{(0)} \cos\frac{\pi x}{2}} \cos\frac{\pi x}{2} dx}{\left(2\int_0^1 e^{\sqrt{2}\, a_1^{(0)} \cos\frac{\pi x}{2}} dx\right)^p} = 0. \tag{4.7}$$

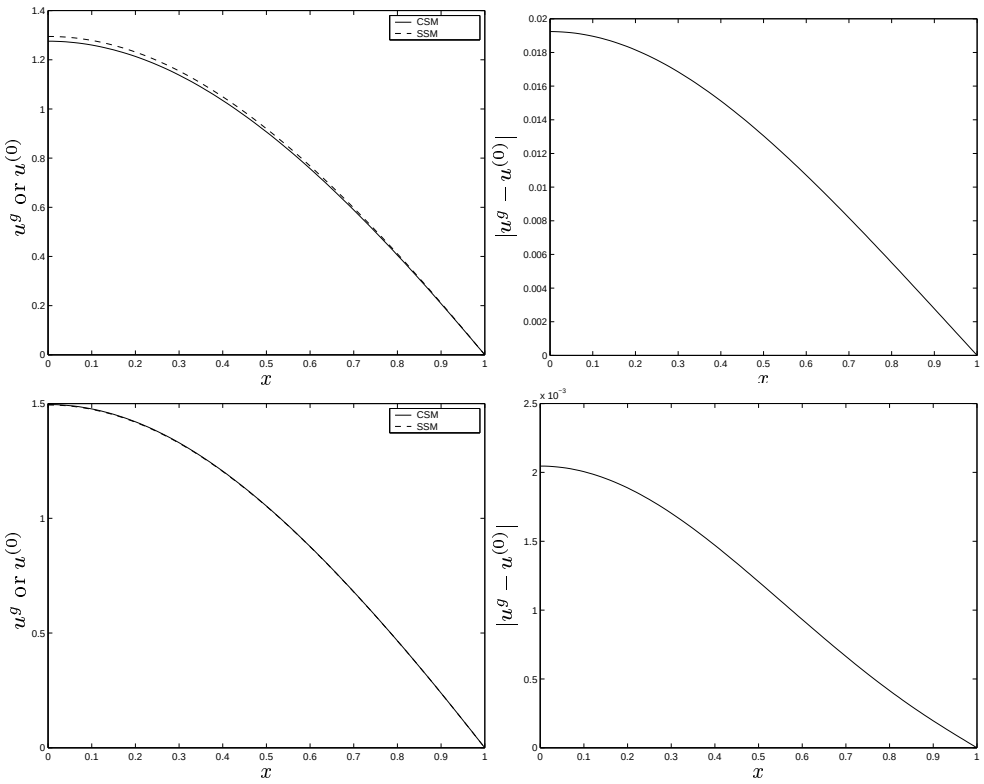

Figure 4.5: Comparison of u^c and $u^{(0)}$, and the difference $|u^c - u^{(0)}|$ for the first and second solution for $p = 1/6$ and $\delta = 1.14$.

This equation has two solutions $a_1^{(0)}$ for $0 \leq p < 1$, if $\delta < \delta^*$, immediately indicating multiple solutions, since each value of $a_1^{(0)}$ can generate an expansion. This would be much more difficult to detect in the CSM. By plotting the graphs of equation (4.7) for different values of δ in Figure 4.4 for $p = 1/6$, we observe that equation (4.7) has two solutions for $a_1^{(0)}$, if δ is smaller than some critical value δ^*, and that the two solutions come closer and closer together as δ approaches δ^* from the left. They merge eventually into one solution at $\delta = \delta^*$ and for bigger values of δ there is no solution.

We computed the two solutions of the problem (4.6) for $p = 1/6$ and $\delta = 1.14$ by the CSM and the SSM. A comparison of the coefficients $a_j^{(n)}$ and a_j is given in Table 4.4. Here again the initial coefficients $a_j^{(0)}$ are not far from the classical spectral coefficients a_j, but the SSM takes now more iterations to converge. Figure 4.5 shows the solutions u^c, $u^{(0)}$, and the difference $|u^c - u^{(0)}|$ between the two approximate solutions.

The computation time depends on the nature of the nonlinearity in the problem, N, and the nonlinear solver used. In the SSM, we only have to solve scalar equations regardless of the value of N, whereas in the CSM, the computation time depends very much on the system size N. In addition, for solving a system of N equations, a good

	first solution			second solution		
	CSM	SSM		CSM	SSM	
j	a_j	$a_j^{(0)}$	$a_j^{(70)}$	a_j	$a_j^{(0)}$	$a_j^{(63)}$
1	0.904836965	0.918163001	0.904836965	1.056103439	1.054778681	1.056103439
2	-0.004699530	-0.004422257	-0.004699530	-0.000228582	-0.000357669	-0.000228582
3	0.002457131	0.002460107	0.002457131	0.002430340	0.002439498	0.002430340
4	-0.000902004	-0.000900857	-0.000902004	-0.000865839	-0.000868569	-0.000865839
5	0.000430335	0.000429725	0.000430335	0.000416076	0.000416994	0.000416076
6	-0.000237206	-0.000236814	-0.000237206	-0.000229851	-0.000230235	-0.000229851
7	0.000144341	0.000143966	0.000144341	0.000140093	0.000140128	0.000140093

Table 4.4: Comparison of the coefficients of the first and second solution obtained by the CSM and the SSM for $p = 1/6$ and $\delta = 1.14$.

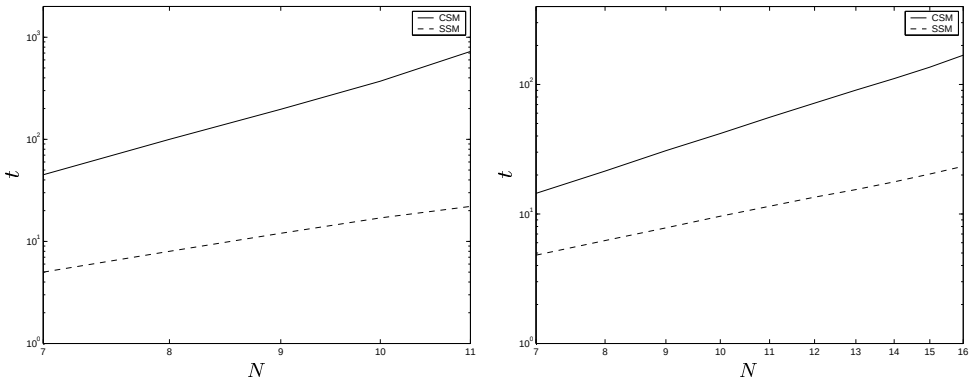

Figure 4.6: Comparison of the computation time measured in seconds for the CSM and the SSM for $p = 1$, $\delta = 1$ and different values of N. On the left for Maple, the approximate slope for the CSM is 6.086 and for the SSM it is 3.381. On the right for Matlab, the approximate slope for the CSM is 2.951 and for the SSM it is 1.888.

initial guess is crucial. Using the initial guess $a_j^{(0)}$ computed with the SSM for a_j, the computation time decreases, but is still significantly higher than the time taken by the SSM for $N = 7$. In addition the ratio of computation time of the SSM and the CSM increases as we increase N. Figure 4.6 shows on the left a comparison of the time taken by the SSM and the CSM in a Maple implementation for $p = 1$, $\delta = 1$, using as an initial guess the one computed by the SSM, and different values of N. Here computation time is the time taken by using the nonlinear equation solver in Maple for both the CSM and the SSM. Using the method of least squares, the approximate slopes for the CSM and the SSM are 6.086 and 3.381 respectively. This means that the approximate computational complexity in Maple for this problem for the CSM is $t_c \approx N^{6.1}$ and for the SSM it is $t_s \approx N^{3.4}$. We also solved the same problem using the nonlinear equation solver in Matlab with tolerance $1e-10$, and measured the computation time for the CSM and SSM for different values of N. Figure 4.6 shows on the right a comparison of the time taken by the SSM and the CSM using zero as an

p	δ^*	p	δ^*
0.00	[0.8773,0.8774]	0.60	[2.7456,2.7457]
0.04	[0.9327,0.9328]	0.70	[3.6693,3.6694]
0.08	[0.9930,0.9931]	0.75	[4.3724,3.2725]
0.10	[1.0251,1.0252]	0.80	[5.3903,5.3904]
0.20	[1.2087,1.2088]	0.90	[10.232,10.233]
0.25	[1.3179,1.3180]	0.92	[12.596,12.597]
0.30	[1.4417,1.4418]	0.94	[16.501,16.502]
0.40	[1.7454,1.7455]	0.96	[24.238,24.239]
0.50	[2.1567,2.1568]	0.98	[47.229,47.230]

Table 4.5: Range for the values of δ^* for different values of p.

initial guess. Using least squares, the approximate slopes for the CSM and the SSM are 2.951 and 1.888 respectively. This means that the approximate computational complexity in Matlab for this problem for the CSM is $t_c \approx N^3$ and for the SSM it is $t_s \approx N^{1.9}$. These results indicate that the nonlinear solver in Matlab is better for this problem than the nonlinear solver of Maple. Nevertheless the computational advantage of the SSM over the CSM persists for the two very different nonlinear black box solvers.

If $0 \leq p < 1$, then by Theorem 4.1, there exists a value δ^*, such that the boundary value problem (4.6) has no solution for $\delta > \delta^*$. With the SSM, we can estimate the critical value δ^* by examining equation (4.7) numerically. The estimates for δ^* for different values of p are given in Table 4.5. These estimates are very difficult to find with a CSM. This is a big advantage of the SSM: the behavior of the solution can be estimated by examining a single scalar equation instead of solving a system of N equations in the CSM.

5. Concluding Remarks. We presented and analyzed the sequential spectral method (SSM) for nonlinear integro-differential equations of elliptic type. We proved that the method converges linearly and the convergence rate depends on the ratio of the Lipschitz constant of the nonlinear function and the first eigenvalue of the elliptic operator. The SSM has several advantages over the CSM: one needs to solve only scalar nonlinear algebraic equations instead of a system of nonlinear equations, one can continue to add components until the required accuracy is reached while the process is running, the existence of multiple solutions can be detected, the dependence of the solution on parameters can be analyzed by studying a single equation, and also estimates for critical values of the parameters can be obtained. In addition the computational cost is significantly lower than for the CSM, and the same solution is obtained.

The SSM has been tested on a variety of applications, both for steady and evolution problems, see [1, 18, 12]. It has even been successfully applied in cases where a convergence analysis is only possible under conditions which are not met in practice [13]. The SSM represents a new and different approach to obtain solutions of classical spectral discretizations for nonlinear problems.

REFERENCES

[1] M. Alrefai. *Sequential Eigenfunction Expansion for Certain Nonlinear Parabolic Systems and Wave Type equations.* PhD thesis, McGill University, June 2000.

[2] M. Alrefai and K. K. Tam. Sequential eigenfunction expansion for a problem in combustion theory. *ANZIAM J.*, 44:35–48, 2003.

[3] C. Baker and C. Philips. *The Numerical Solutions of Nonlinear Problems.* Clarendon Press, Oxford, 1981.

[4] J. Bebernes and A. Bressan. Thermal behavior for a confined reactive gas. *J. Differential Equations*, 44:118–133, 1982.

[5] J. Bebernes, C. Li, and P. Talaga. Single-point blowup for nonlocal parabolic problems. *Physica D*, 134:48–60, 1999.

[6] J. W. Bebernes and A. A. Lacey. Global existence and finite-time blow-up for a class of nonlocal parabolic problem. *Advances in Differential Equations*, 2:927–953, 1997.

[7] J. W. Bebernes and P. Talaga. Nonlocal problems modeling shear banding. *Communications on applied nonlinear analysis*, 3:79–103, 1996.

[8] T. J. Burns. *Connections between Localized Behavior in Plasticity and in Combustion, Material Instabilities–Theory and Application.* The American Society of Mechanical Engineers, 1994.

[9] E. Caglioti, P. L. Lions, C. Marchioro, and M. Pulvirenti. A special class of stationary flows for two-dimensional Euler equations: A statistical mechanics description. *Communications in Mathematical Physics*, 143:501–525, 1992.

[10] C. Canuto, M. Y. Hussaini, A. Quarteroni, and T. A. Zang. *Spectral Methods in Fluid Dynamics.* Springer-Verlog, USA, 1987.

[11] M. J. Gander. *Analysis of Parallel Algorithms for Time Dependent Partial Differential Equations.* PhD thesis, Stanford University, August 1997.

[12] M. J. Gander. A frequency decomposition waveform relaxation algorithm for semilinear evolution equations. *Electronic Transactions on Numerical Analysis (ETNA)*, to appear, 2004.

[13] B. Gwamanda. The sequential spectral method for incompressible Navier-Stokes equations in two dimensions. Master's thesis, McGill University, February 2004.

[14] A. Krzywicki and T. Nadzieja. Some results concerning the Poisson-Boltzmann equation. *Zastosowania Mat. Appl. Math.*, 21:265–272, 1991.

[15] Kuo and Pen-Yu. *Spectral Methods and their Applications.* World Scientific, London, 1998.

[16] A. A. Lacey. Thermal runaway in a nonlocal problem modeling ohmic heating: Part i. *European journal of applied Mathematics*, 6:127–144, 1995.

[17] A. A. Lacey. Thermal runaway in a nonlocal problem modeling ohmic heating: Part ii. *European journal of applied Mathematics*, 6:201–224, 1995.

[18] A. Mansoora. *The Sequential Spectral Method for Integro-Differential Equations.* PhD thesis, McGill University, November 2001.

[19] A. Merchand and J. Duffy. An experimental study of the formation of adiabatic shear bands in a structural steel. *Journal of Mechanical Physics and Solids*, 36:251–283, 1988.

[20] W. E. Olmstead, S. Nemat-Nasser, and L. Ni. Shear bands as surfaces of discontinuity. *Journal of Mech. Phy. Solids*, 42:697–709, 1994.

[21] C. V. Pao. Blowing-up of solutions for a nonlocal reaction-diffusion problem in combustion theory. *J. math. Anal. Appl.*, 166:591–600, 1992.

[22] K. K. Tam, Andonowati, and M. T. Kiang. Nonlinear eigenfunction expansion for a problem in microwave heating. *Canadian Applied Mathematics Quarterly*, 4:311–325, 1996.

[23] K. K. Tam, Andonowati, and M. T. Kiang. Sequential eigenfunction expansion for certain nonlinear Hammerstein equations. *Canadian Applied Mathematics Quarterly*, 9(2):189–202, 2001.

[24] N. L. Trefethen. *Spectral Methods in MATLAB.* Society for Industrial and Applied Mathematics (SIAM), Philadelphia, PA, 2000.